# DNA Length-Dependent Cooperative Interactions in the Binding of Ku to DNA†

Yunmei Ma and Michael R. Lieber*

*Norris Comprehensive Cancer Center, Room 5428, Department of Pathology, Biochemistry & Molecular Biology, Molecular Microbiology & Immunology, and Biological Sciences, University of Southern California Keck School of Medicine, 1441 Eastlake Avenue, Mail Code 9176, Los Angeles, California 90089-9176*

*Received May 7, 2001*

ABSTRACT: Despite its central role in the nonhomologous DNA end joining process, we still have an incomplete picture of the interaction between Ku and DNA. Here we describe both kinetic (surface plasmon resonance or SPR) and equilibrium (electrophoretic mobility shift assay or EMSA) studies of Ku binding to linear double-stranded DNA. Ku interaction with 1-site DNA is noncooperative, as expected. Electrophoretic mobility shift assays indicate cooperativity in the binding of Ku molecules to DNA long enough for two Ku molecules to bind (2-site DNA). For the kinetic studies, we use surface plasmon resonance in which one end of the DNA molecules is linked to a surface while the other end is free to interact with Ku. We find that one Ku molecule dissociates from 1-site DNA with simple Langmuir (i.e., independent) kinetics. However, two Ku molecules associate and dissociate from 2-site DNA with a time course that cannot be described as a simple Langmuir interaction. On 3- and 4-site DNA, EMSA and SPR studies do not reveal any cooperativity, suggesting that the middle Ku does not exhibit cooperative interaction with the two Ku molecules bound at the DNA ends. These results indicate that Ku molecules can demonstrate cooperative interaction, and this is influenced by their positions along the DNA.

Double-stranded (ds)[1] DNA breaks are potentially lethal DNA lesions, and all eukaryotic organisms have evolved enzymatic processes to repair them. Two different sources of such breaks can be distinguished. Physiologic ds DNA breaks are caused by V(D)J recombination and class switch recombination (*1*). Pathologic ds DNA breaks are thought to be caused by oxidative free radicals, ionizing radiation, and endogenous errors of DNA metabolism. There are two major pathways for repairing such breaks in cells of multicellular eukaryotes. Nonhomologous DNA end joining (NHEJ) is the major pathway for ds DNA break repair during G0, G1, and early S phases, whereas homologous recombination is the major pathway during late S and G2 phases (*1*, *2*). Loss of either pathway results in chromosomal instabilities (*3*−*6*). Recent studies indicate that cells suffer spontaneous ds DNA breaks, requiring repair by the NHEJ pathway (*3*).

NHEJ at a ds DNA break is thought to begin with the binding of Ku to each of the two DNA ends at the break site. (Throughout this study, one Ku molecule is defined as being composed of one Ku70 plus one Ku86 polypeptide, such that it exists in its stable heterodimeric form.) The 469-kDa DNA-PK (often called DNA-PK$_{cs}$) binds to the Ku:DNA complex. The interaction of Ku and the 469-kDa DNA-PK is dependent on the association of Ku with DNA (*7*, *8*). Once the Ku:DNA-PK complex slides a sufficient distance internally onto the DNA end, the protein kinase activity of the 469-kDa DNA-PK is activated (*8*). It is not clear which proteins the 469 kDa DNA-PK functionally phosphorylates during NHEJ. The subsequent steps of the process are also unclear. The broken DNA ends must be modified by nucleases and polymerases into ligatable DNA ends. The first genetically implicated 5′ nuclease for this process is FEN-1, which would act after the two ends have annealed at chance sites of terminal microhomology (*9*). A genetically implicated polymerase is POL4 (the *Saccharomyces cerevisiae* homologue of mammalian polymerase $\beta$) (*10*). Recently, a biochemical interaction between Ku and the Werners protein (WRN) was established (*11*, *12*). WRN is a 3′ nuclease and a helicase. All possible DNA ends can be processed into ligatable configurations with a 5′ nuclease, a 3′ nuclease, and a polymerase. The final step is ligation, which is performed by the XRCC4/DNA ligase IV complex for all NHEJ events in all eukaryotic organisms (*13*−*15*).

The largest genetic effects on the NHEJ pathway are observed for XRCC4, DNA ligase IV, Ku70, and Ku86. It is clear that the XRCC4/DNA ligase IV complex performs the ligation step. However, the role of Ku in NHEJ remains to be explained. Previous studies from our laboratory showed that Ku improves the equilibrium binding affinity of the 469-kDa DNA-PK by about 100-fold (*8*). Genetic studies suggest that Ku does more than simply stabilize the binding of the 469-kDa DNA-PK (*16*). For example, in V(D)J recombination, the phenotype of Ku null mutants is different than that of DNA-PKcs null mutants (*17*, *18*). In yeast, Ku acts independently of the 469 kDa DNA-PK because the latter does not exist in yeast. These differences indicate that Ku serves roles independent of the 469-kDa DNA-PK.

The interaction of Ku alone with DNA has been the subject of previous studies, the earliest of which demonstrated that Ku binds at ds DNA ends (*19*−*22*). Studies of the affinity

† This work was supported by NIH grants. M.R.L. is the Rita & Edward Polusky Basic Cancer Research Professor.

* Corresponding author: Phone 323-865-0568, Fax 323-865-3019, E-mail lieber@usc.edu.

[1] Abbreviations: SPR: surface plasmon resonance; EMSA: electrophoretic mobility shift assay; ds: double-stranded; NHEJ: nonhomologous end joining; DNA-PK$_{cs}$: DNA-dependent protein kinase, catalytic subunit.

10.1021/bi010932v CCC: $20.00 
Published on Web 07/20/2001

of Ku for various DNA configurations demonstrated that Ku binding is specific for single- to double-strand transitions (*23*, *24*). After loading at DNA ends, Ku can diffuse to internal positions in an energy-independent manner (*22*). At 4 °C, it was demonstrated that Ku can move from one linear DNA to another, across transient base pairings of the DNA termini (*25*). Ku is associated with the telomeres in yeast (*26*, *27*) and in mammalian cells (*28*). Though some studies have indicated that Ku may be a helicase (*29*), others have not confirmed this (*11*). Many questions remain concerning the interaction of Ku with DNA, especially when the DNA length is sufficient for more than one Ku molecule to load.

Here we have used electrophoretic mobility shift assays (EMSA) and surface plasmon resonance (SPR) kinetic approaches to examine the interaction of Ku with linear DNA ranging in size from 1 site to 4 sites in length. Interaction of Ku with a DNA molecule able to accommodate only one Ku molecule (1-site DNA) demonstrates simple Langmuir (i.e., independent) binding behavior. However, kinetic data on longer DNA molecules able to accommodate two Ku molecules (2-site DNA) cannot be described by independent site binding. EMSA analysis on 2-site DNA indicates that a second Ku molecule can bind with an equilibrium association constant that is nearly 14-fold greater than that of the first Ku, thus demonstrating cooperative behavior. Studies with longer DNA (3- and 4-site DNA) suggest that internally positioned Ku molecules are not cooperative. This information about the cooperativity and the differences between terminal and internal Ku molecules provides structural insight into the architecture of the DNA repair complex in NHEJ.

## EXPERIMENTAL PROCEDURES

*Oligonucleotides.* The oligonucleotides were synthesized (Operon Technology, Alameda, CA, or Microchemical Core Facilities, Norris Cancer Center, USC) and the sequences are as follows (blunt; only top strand shown): 18 bp (YM-28), 5′-AGGCTGTGTCCTCAGAGG-3′; 22 bp (YM-2), 5′-AGGCTGTGTTAGCCCTCAGAGG-3′; 45 bp (YM-6), 5′-AGGCTGTGTTAAGTATCTGCATCGGATCGGGC-TCGCCCTCAGAGG-3′; 68mer (YM-44), 5′-AGGCTGT-GTTAAGTATCTGCATCTTACTTGACGGTACTGGT-CAAGCGGATCGGGCTCGCCCTCAGAGG-3′; and 90 bp (YM-46), 5′-AGGCTGTGTTAAGTATCTGCATCTTACT-TGACGGATGCAATCGTCACGTGCTAGACTACTGGT-CAAGCGGATCGGGCTCGCCCTCAGAGG-3′. The sequence of the longer oligonucleotides was designed by inserting nucleotides into the middle of the immediate shorter one so that the ends of the ds oligonucleotides stay the same for Ku to recognize. In addition to YM-6, three other sequences for the 45bp DNA were used. The sequences are as follows (only top strand shown): YM-59, 5′-AGGCT-GTGTTAAGTATCTGCATCCTAGGTGACCGTAGCTC-TATAG-3′; YM-61, 5′-CTGACCTAGCTAGTCAAGCTG-GAGGATCGGGCTCGCCCTCAGAGG-3′; YM-63, 5′-CTGACCTAGCTAGTCAAGCTGGACTAGGTGAC-CGTAGCTCTATAG-3′. Complementary single-stranded oligonucleotides were purified by denaturing polyacrylamide gel electrophoresis and annealed in 10 mM Tris-Cl, pH 8.0, 1 mM EDTA, 100 mM NaCl by boiling for 5 min (in a 500-mL beaker containing 400-mL of water), followed by slow cooling of the entire beaker down to room temperature over a period of several hours, and subsequent transfer to 4 °C.

*Purification of Ku.* Recombinant Ku was expressed in Hi5 cells (Invitrogen, Carlsbad, CA) and purified as described (*30*) with the following modifications. The cells were harvested and the cellular extract was obtained by sonication. The supernatant was purified over Ni−NTA agarose (Qiagen, Valencia, CA), and then applied to a ds DNA Sepharose column (prepared according to Amersham Pharmacia Biotech manual). Finally, the Ku protein was purified over a Mono Q column (Amersham Pharmacia Biotech, Piscataway, NJ). Ku containing fractions (identified by Western blotting) were collected, and the protein concentration was determined by calculating the extinction coefficient from the amino acid composition (based on tryptophan and tyrosine residues) and measuring the absorbance of the purified protein in 6 M guanidine HCl at 280 nm.

*Electrophoretic Mobility Shift Assay (EMSA).* Before annealing the two complementary oligonucleotides, one strand was radioactively labeled with T4 polynucleotide kinase (New England Biolabs, Beverly, MA), and then annealed to the other strand. In a 20 $\mu$L reaction, various amounts of Ku were mixed with 0.5 nM of DNA probe in 40 mM HEPES, pH 7.6, 125 mM KCl, 10 mM $MgCl_2$, 5 mM DTT, 0.5 mM EDTA, 10% glycerol, and 0.1 mg/mL BSA at room temperature for 10 (for binding to 18 bp, 22 bp, and 45 bp ds DNA oligonucleotides) or 20 min (for binding to 68 and 90 bp ds DNA oligonucleotides).

After incubation, the reaction mixtures were loaded onto a 5% nondenaturing polyacrylamide gel and run at 9 V/cm at room temperature in 1× TBE buffer. The gel was then dried, exposed to a PhosphorImager screen (Molecular Dynamics, Sunnyvale, CA), and quantitated by using ImageQuant software (version 1.1 and 5.0).

The dissociation constant ($K_D$) from the Ku EMSA experiments was calculated as described (*31*).

*Simultaneous Binding Model and Data Analysis.* The simultaneous binding model can be described as:

$$h\text{Ku} + \text{DNA} \overset{K_D{}^h}{\longleftrightarrow} \text{Ku}_h\text{:DNA}$$

DNA in our case is treated as a macromolecule that can be bound by one or more Ku molecules, depending on its length. Since the footprinting data suggested that the Ku binding site is approximately 20 bp (*22*, *32*), the 18 bp and 22 bp DNAs were treated as 1-site containing DNAs, the 45 bp DNA was treated as a 2-site DNA, the 68 bp DNA was treated as a 3-site DNA, and the 90 bp was treated as a 4-site DNA. $K_D$ is the intrinsic dissociation constant of Ku without cooperativity or the $K_D$ of Ku upon binding to a one-site DNA molecule. The Hill coefficient, *h*, is used as the index of cooperativity, and *h* does not have to be an integer. The relationship between *h* and the cooperativity of a binding reaction is as follows: $0 < h < 1$ indicates negative cooperativity; $h = 1$ indicates no cooperativity; $1 < h < n$ indicates positive cooperativity (or simply referred to as cooperativity) (*n* is the maximum number of Ku molecules that can bind to a DNA molecule in our case).

According to the theory of Hill (*33*), the ratio of occupied sites versus total sites on DNA (or fractional saturation, represented by "*Y*") can be expressed as the function of the concentration of free Ku and $K_D$: $Y = [\text{free Ku}]^h/(K_D + [\text{free Ku}]^h)$. After rearrangement, the equation $\log(Y/(1 - Y)) =$

$h$ log[free Ku] − log$K_D$ ([free Ku] represents the concentration of the free Ku protein at equilibrium) can be used to evaluate the cooperativity of Ku binding to a DNA molecule.

In each experiment with a certain DNA species, a series of binding reactions with a constant DNA concentration and increasing Ku concentrations were set up. After incubation, the reaction mixtures were loaded onto a native polyacrylamide gel. On the gel image, the intensity of different Ku and DNA species was quantitated, and $Y$ is calculated as the ratio of the weighted sum of the amount of Ku:DNA complexes to the amount of total DNA probe. Taking Ku binding to a 45 bp DNA as an example, for each reaction, $Y$ = (2Ku(2) + Ku(1))/(2(Ku(2) + Ku(1) + free probe)). Here Ku(2) represents the band intensity of the complex composed of two Ku molecules and one 45 bp DNA molecule, Ku(1) represents the band intensity of the complex composed of one Ku molecule and one 45 bp DNA molecule, and "free probe" is the intensity of the free probe band. Given each $Y$ value, [free Ku] is calculated as [free Ku] = [total Ku] − 2 × $Y$ × [total DNA] for each reaction with a different total Ku concentration. A plot of log($Y$/(1 − $Y$)) versus log[free Ku] was generated and fit to a linear model. The slope of the best-fit line indicates the cooperativity of Ku binding to this DNA molecule as described above.

*Sequential Binding Model, Curve Fitting, and Data Analysis.* Curve fitting with this model was applied to the results of Ku binding to the 45 bp DNA (2-site molecule) to determine the relative fit of this model versus the fit of the simultaneous model. In this model, the binding of two Ku proteins to one molecule of 45 bp DNA was dissected into two steps:

$$\mathrm{Ku} + \mathrm{DNA} \overset{K_1}{\longleftrightarrow} \mathrm{Ku{:}DNA}$$

$$\mathrm{Ku} + \mathrm{Ku{:}DNA} \overset{K_2}{\longleftrightarrow} \mathrm{Ku_2{:}DNA}$$

where $K_1$ and $K_2$ are intrinsic association constants of the two steps. By definition, $K_1$ = [Ku:DNA]/[Ku] × [DNA] and $K_2$ = [Ku$_2$:DNA]/[Ku] × [Ku:DNA], where [Ku] is the concentration of free Ku protein.

Similar to the fractional saturation, $Y$, the ratio of the average concentration of the bound protein to the concentration of total DNA can be expressed as a dependent variable. Thus,

$$\frac{[\overline{\mathrm{Ku_{bound}}}]}{[\mathrm{DNA_{total}}]} = \frac{[\mathrm{Ku{:}DNA}] + 2 \times [\mathrm{Ku_2{:}DNA}]}{[\mathrm{DNA}] + [\mathrm{Ku{:}DNA}] + [\mathrm{Ku_2{:}DNA}]} \quad (1)$$

From the expressions of $K_1$ and $K_2$, [Ku:DNA] = $K_1$ × [Ku] × [DNA] and [Ku$_2$:DNA] = $K_2$ × [Ku] × [Ku:DNA] = $K_1$ × $K_2$ × [Ku]$^2$ × [DNA]. Consider a cooperativity factor "$c$" and define $c$ as $K_2/K_1$. Thus, if $c$ is greater than 1, the second Ku molecule binds to DNA with a higher affinity than the first one does. Alternatively stated, if $c$ > 1, Ku binds to the 45 bp DNA cooperatively. [Ku$_2$:DNA] can be expressed as $c \times K_1^2 \times [\mathrm{Ku}]^2 \times [\mathrm{DNA}]$. The expressions of [Ku:DNA] and [Ku$_2$:DNA] can be introduced into eq 1 to generate eq 2:

$$\frac{[\overline{\mathrm{Ku_{bound}}}]}{[\mathrm{DNA_{total}}]} = \frac{[\mathrm{Ku{:}DNA}] + 2 \times [\mathrm{Ku_2{:}DNA}]}{[\mathrm{DNA}] + [\mathrm{Ku{:}DNA}] + [\mathrm{Ku_2{:}DNA}]} = \frac{K_1 \times [\mathrm{Ku}] + 2 \times c \times K_1^2 \times [\mathrm{Ku}]^2}{1 + K_1 \times [\mathrm{Ku}] + c \times K_1^2 \times [\mathrm{Ku}]^2} \quad (2)$$

In the above derivation, the DNA molecule was treated as a 2-site binding molecule. However, since DNA is composed of nearly identical repeating units (nucleotides), there potentially could be more binding sites for Ku because Ku can translocate energy independently on DNA. This DNA gridding effect will increase the apparent association constant of the first Ku binding to DNA (*34*), since when the second Ku is to be bound, there is only enough room for one protein. For example, suppose Ku has a minimum site size of 20 bp, a 45 bp DNA potentially has 26 binding sites for one Ku molecule. A factor "$g$" can be introduced, and $g$ is the increase over the intrinsic association constant of the first bound Ku molecule. Thus, eq 2 can be modified to:

$$\frac{[\overline{\mathrm{Ku_{bound}}}]}{[\mathrm{DNA_{total}}]} = \frac{[\mathrm{Ku{:}DNA}] + 2 \times [\mathrm{Ku_2{:}DNA}]}{[\mathrm{DNA}] + [\mathrm{Ku{:}DNA}] + [\mathrm{Ku_2{:}DNA}]} = \frac{g \times K_1 \times [\mathrm{Ku}] + 2 \times c \times K_1^2 \times [\mathrm{Ku}]^2}{1 + g \times K_1 \times [\mathrm{Ku}] + c \times K_1^2 \times [\mathrm{Ku}]^2} \quad (3)$$

Fitting of experimental data to eq 3 was carried out using the software KaleidaGraph (v3.0). We found that the optimal fit of the sequential model to the EMSA data is for a site size of two ($g$ = 2). Therefore, in the curve fitting iteration, $g$ was fixed at 2.

*Surface Plasmon Resonance (SPR).* The binding reactions were carried out in a BIACORE X instrument (Biacore Inc., San Diego, CA) in 84 mM $K_2HPO_4$, 52 mM $KH_2PO_4$, (pH 7.0), 10 mM $NaHCO_3$, 1 mM $MgSO_4$, 4 mM KCl, 10% glycerol, 2 mM DTT, 0.5 mM EDTA, and 0.005% Surfactant P20 (Biacore, Inc.) at 25 °C unless specified. The 5′-biotinylated ds oligonucleotides were immobilized onto a streptavidin-coated chip surface (Sensor chip SA, Biacore, Inc.). (DNA that has a terminal biotin, and which is bound to streptavidin, has been previously shown not to load Ku from that end (*35*).) The amount of DNA added was such that the subsaturation level of Ku bound was 50 to 100 response units. Then Ku was diluted in the running buffer and injected onto the DNA surface at a flow rate of 90 $\mu$L/min to minimize any possible mass transfer effect. (Mass transfer effects were tested for by slowing the flow rate to 10 $\mu$L/min; this did not have an effect on the kinetics. However, mass transfer may play a role on some chips, where indicated.) Ku was allowed first to flow through a control cell lacking immobilized DNA, and then through an experimental flow cell containing DNA of interest. The association phase was usually 47 s and was followed by a dissociation phase (120 s or longer) in which running buffer flowed over the protein−DNA surface. After each injection of protein, the surface was regenerated by a one-minute injection of 0.05% SDS or 2 M KCl. The responsive difference of the experimental and control cell, expressed in an arbitrary unit "response unit", was monitored as a function of time. To obtain kinetic parameters, late association phases (about 70% of the total association phase) and

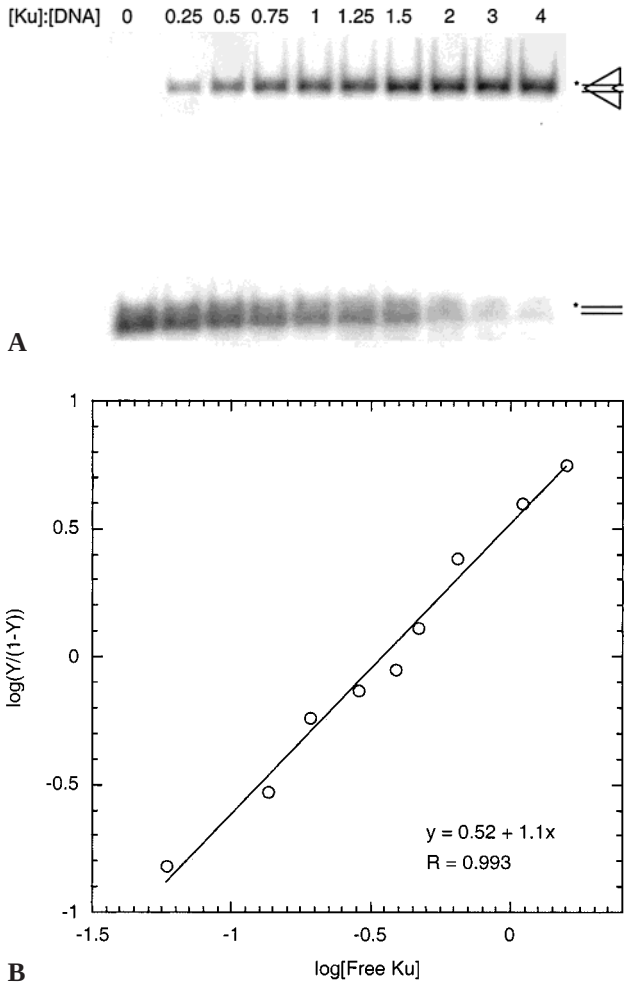


FIGURE 1: Ku binding to 18 bp ds DNA reflects simple Langmuir binding. (A) EMSA of Ku binding to an 18 bp DNA. The DNA concentration is 0.5 nM in all binding reactions, and the Ku concentrations are reflected by the Ku to DNA ratios. Positions of the free probe and Ku:DNA complex are indicated. Ku is depicted by a triangle with a recessed notch on one side (tail). (B) The Hill plot of the Ku EMSA (Figure 1A) with the 18 bp DNA as a probe (see text). The formula represents the best-fit line for the data, and "R" is the regression coefficient. The slope of the line, 1.1 in this case, is the Hill coefficient.

early dissociation phases (40 to 130 s) of the resulting sensorgrams were fit to the Langmuir binding model using BIAevaluation software (version 3.0). This is recommended because refractive index changes complicate the early portion of the association phase and because rebinding complicate the later portion of the dissociation phase.

## RESULTS

*Ku Binds to an 18 or 22 bp ds DNA Fragment with Simple Langmuir Binding Kinetics.* As part of an effort to dissect the early events in the NHEJ pathway, we sought a quantitative assessment of the interaction of Ku with DNA fragments of various lengths. As our initial choice for analysis, we chose blunt linear ds DNA fragments of 18 or 22 bp, because 20 bp is approximately the unit site size for Ku binding based on previous work from our laboratory and others (*22*, *32*).

Our initial method of analysis was EMSA using the 18 bp ds DNA oligonucleotide (Figure 1A). We varied the concentration of recombinant Ku over a range from 0.13 to 2.0 nM, while the DNA concentration was fixed at 0.5 nM. We observed only one Ku shifted species, consistent with the expectation that 18 bp is only long enough to accommodate one Ku molecule. Graphical analysis (*31*) indicates that 50% of the 18 bp ds DNA is bound by Ku at a concentration of 0.38 nM free Ku, indicating that this is the approximate $K_D$. A double logarithmic plot (Hill plot) of these data was done in which $\log(Y/(1 - Y))$ was plotted as a function of log[free Ku] (see Experimental Procedures) (Figure 1B). The slope of this plot is 1.1, indicating that there is no cooperativity (*33*), as expected for 1-site DNA.

Table 1: Summary of Hill Coefficients of Ku Binding to DNA

| | 45 bp DNA[a] | | 22 bp DNA | | 18 bp DNA | |
|---|---|---|---|---|---|---|
| exp | Hill coefficient | *r* | Hill coefficient | *r* | Hill coefficient | *r* |
| 1 | 1.65 | 0.992 | 0.84 | 0.957 | 0.68 | 0.973 |
| 2 | 1.56 | 0.962 | 1.00 | 0.996 | 1.13 | 0.993 |
| 3 | 1.55 | 0.994 | 1.10 | 0.996 | | |
| 4 | 1.55 | 0.993 | | | | |
| 5 | 1.51 | 0.985 | | | | |
| 6 | 1.27 | 0.984 | | | | |
| 7 | 1.44 | 0.984 | | | | |
| 8 | 1.82 | 0.969 | | | | |
| 9 | 1.85 | 0.990 | | | | |
| mean ± SD | 1.58 ± 0.18 | | 0.98 ± 0.13 | | 0.91 ± 0.32 | |

[a] For EMSA with 45 bp DNA as probe, experiments 1 to 6 were done with YM-6 and its complementary oligonucleotide; experiments 7 to 9 were done with YM-59, YM-61, YM-63 and their complementary oligonucleotides, respectively.

We repeated these studies with a blunt-ended oligonucleotide of 22 bp and obtained comparable Hill coefficient and $K_D$ values as those for the 18 bp DNA (Table 1 and data not shown).

In addition to EMSA, we used SPR to examine the kinetics of Ku interaction with the 18 bp ds DNA. In this method, we linked the 18 bp ds DNA fragment to the surface of a streptavidin-coated chip using a 5′ terminal biotin derivative. Ku is then allowed to flow through the surface upon which the ds DNA is immobilized. We find that Ku binds to 18 bp ds DNA in a 1:1 manner with a dissociation constant of $1.4 \times 10^{-9}$ M (shown by the small chi square value upon fitting the data to a 1:1 Langmuir binding model in BIAevaluation 3.0) (Figure 2A and Table 2).

We repeated the SPR study using a 22 bp DNA 5′ terminally linked to the SPR surface. The sequence of the 22 bp DNA was the same as that of the 18 bp DNA except for the addition of 4 bp in the middle of the sequence. Our results were similar in that the kinetics could be fit with a simple Langmuir binding model (Figure 2B and Table 2). The off-rate was slower, and the resulting equilibrium dissociation constant was about 10-fold lower ($K_D = 1.6 \times 10^{-10}$), which is comparable to the calculated constant using EMSA for the 18 and 22 bp DNAs (data not shown).

On the basis of both the EMSA and SPR results, we infer that Ku interacts with short DNA (blunt 18 bp and 22 bp ds DNA) with simple 1:1 Langmuir kinetics, according to the following equation:

$$\text{Ku} + \text{DNA} \overset{K_D}{\longleftrightarrow} \text{Ku:DNA}, \text{ where } K_D = \frac{[\text{Ku}][\text{DNA}]}{[\text{Ku:DNA}]}$$

*Ku Binds to a 45 bp ds DNA in a Cooperative Manner Based on EMSA.* We were interested in confirming the

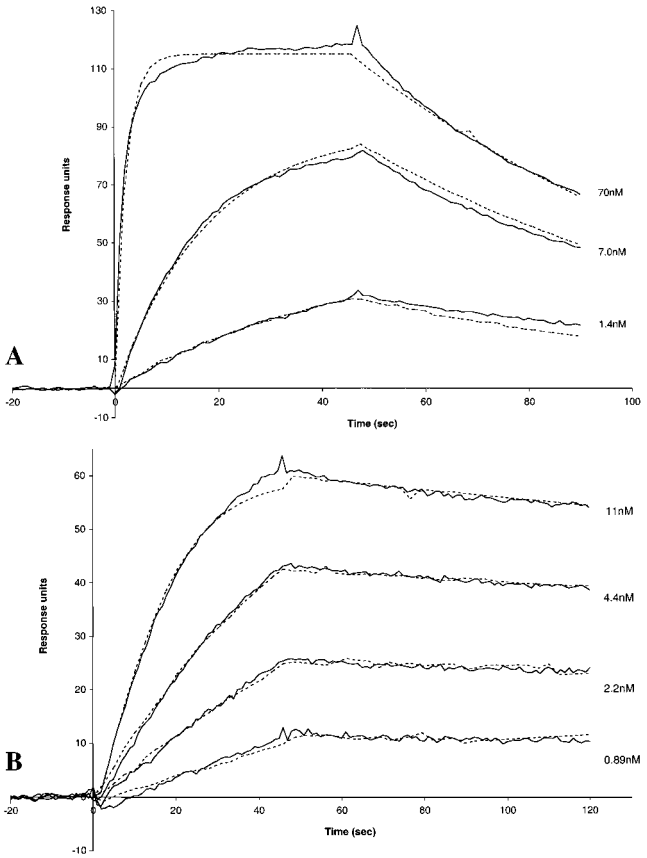


FIGURE 2: Ku binding to 1-site DNA by SPR indicates simple Langmuir interaction. (A) Sensorgram of Ku binding to an 18 bp DNA which is linked to the sensor chip surface at the end. Single runs of three Ku concentrations (70, 7.0, and 1.4 nM) are shown. Each curve was repeated in a duplicate experiment with similar results (data not shown). Dashed lines indicate the best-fit curves. (B) Sensorgram of Ku binding to a 22 bp DNA which is linked to the sensor chip surface at the end. Single runs of four Ku concentrations (11, 4.4, 2.2, and 0.89 nM) are shown. Dashed lines indicate the best-fit curves. The dissociation phase was shortened for simplicity since this had no effect on the best-fit kinetic values. Biacore software curve-fitting program emphasizes the later portion of the association phase and the early portion of the dissociation phase.

binding properties of Ku at longer DNA lengths. We carried out EMSA in the same manner as for the 18 and 22 bp ds DNA, except for using a 45 bp DNA fragment (Figure 3A). We observed two shifted bands, corresponding to one and two Ku molecules bound to the 45 bp DNA. This is consistent with our studies and those of others concerning the approximate length of DNA required for binding a single Ku molecule. A Hill plot of the results showed that the Hill coefficient is 1.51 (Figure 3B). Multiple experiments (Table 1) indicate that the Hill coefficient of Ku binding to 45mer has an average value of 1.6, and this is significantly higher than the mean of 0.9 or 1.0 that we observed for the 18 bp or 22 bp ds DNA. This suggests that Ku binds cooperativelyto DNA when that DNA has sufficient length to accommodate two Ku molecules.

We were interested in whether the distinctive cooperative binding of Ku to 2-site DNA is a general property of 2-site DNA or specific to this particular 2-site sequence. We therefore repeated the binding studies with three additional 2-site DNA molecules, all of different sequence from that used above. All three of the additional 2-site DNA molecules bound Ku cooperatively (Table 1, experiments 7 to 9).

We were interested in also analyzing the binding of Ku to DNA according to a sequential binding model. This is in contrast to the model that is intrinsically assumed in Hill plots, which is based on simultaneous binding. Simultaneous models (as in Hill plots) are based on the following type of equation:

$$h\mathrm{Ku} + \mathrm{DNA} \overset{K_D^h}{\longleftrightarrow} \mathrm{Ku}_h\mathrm{:DNA} \text{ (where } h \leq 2)$$

In contrast, in a sequential binding model for the 45 bp ds DNA, one assumes the following:

$$\mathrm{Ku} + \mathrm{DNA} \overset{K_1}{\longleftrightarrow} \mathrm{Ku:DNA}$$

$$\mathrm{Ku} + \mathrm{Ku:DNA} \overset{K_2}{\longleftrightarrow} \mathrm{Ku}_2\mathrm{:DNA}$$

where $K_2 = cK_1$ and $c$ is the cooperativity factor.

For the sequential model, we plotted the data on a graph of $[\overline{\mathrm{Ku}_{\mathrm{bound}}}]/[\mathrm{DNA}_{\mathrm{total}}]$ on the ordinate and [free Ku] on the abscissa (see Experimental Procedures). We found that this model fits the observed data (Figure 3A) well when we keep $K_1$ and $c$ as unknown constants (see Experimental Procedures) (Figure 3C). In the best fit equation, $K_1$ was $5.2 \times 10^8$ and $c$ was 13.7, which indicates that the second Ku binds to the complex of $\mathrm{Ku}_1$:DNA with an equilibrium association constant that is 13.7-fold greater than that of the first Ku. Like the Hill model data analysis, the sequential model also indicates cooperativity in the binding of Ku to DNA.

Given the unusual contrast in binding properties of Ku as a function of linear ds DNA length, we were interested in obtaining more detailed binding information using an independent method. We used SPR analysis for the 45 bp ds DNA fragment, and, as in the case of the 18 bp ds DNA, the linear DNA was attached to the surface of the SPR chip using a terminal biotin linkage. We find that the association and dissociation kinetics for Ku with 45 bp DNA differ from that of the 18 and 22 bp DNA (Figure 4). Current SPR data analysis programs cannot be readily applied to cooperative interactions. We can only determine that the kinetics are inconsistent with a simple Langmuir binding model.

*EMSA and SPR Analysis of Ku Binding to 3- and 4-Site DNA.* We performed the EMSA analysis on 3- and 4-site linear ds DNA oligonucleotides to determine if the cooperative binding was apparent at these lengths. We determined that the blunt 68 bp DNA indeed binds three and no more than three Ku molecules. Likewise, the 4-site DNA, which is 90 bp in length, binds four and no more than four Ku molecules (data not shown). However, we find that on both of these DNAs, the Hill plots have slopes between 0.96 and 1.25 (data not shown). Note that the terminal DNA sequences for the 68 and 90 bp DNAs are identical to those for the shorter DNAs. On the basis of the relatively noncooperative nature of the EMSA data for 3- and 4-site DNA, we infer that the middle Ku molecules may not maintain the cooperative interaction that two terminally bound Ku molecules can achieve on a 2-site DNA molecule (Figure 5A). Alternatively, the complexity of the system (the large number of possible cooperative and noncooperative interactions) may make it difficult to detect any cooperativity.

We also extended our SPR analysis by examining the binding kinetics for a ds DNA fragment to which three Ku

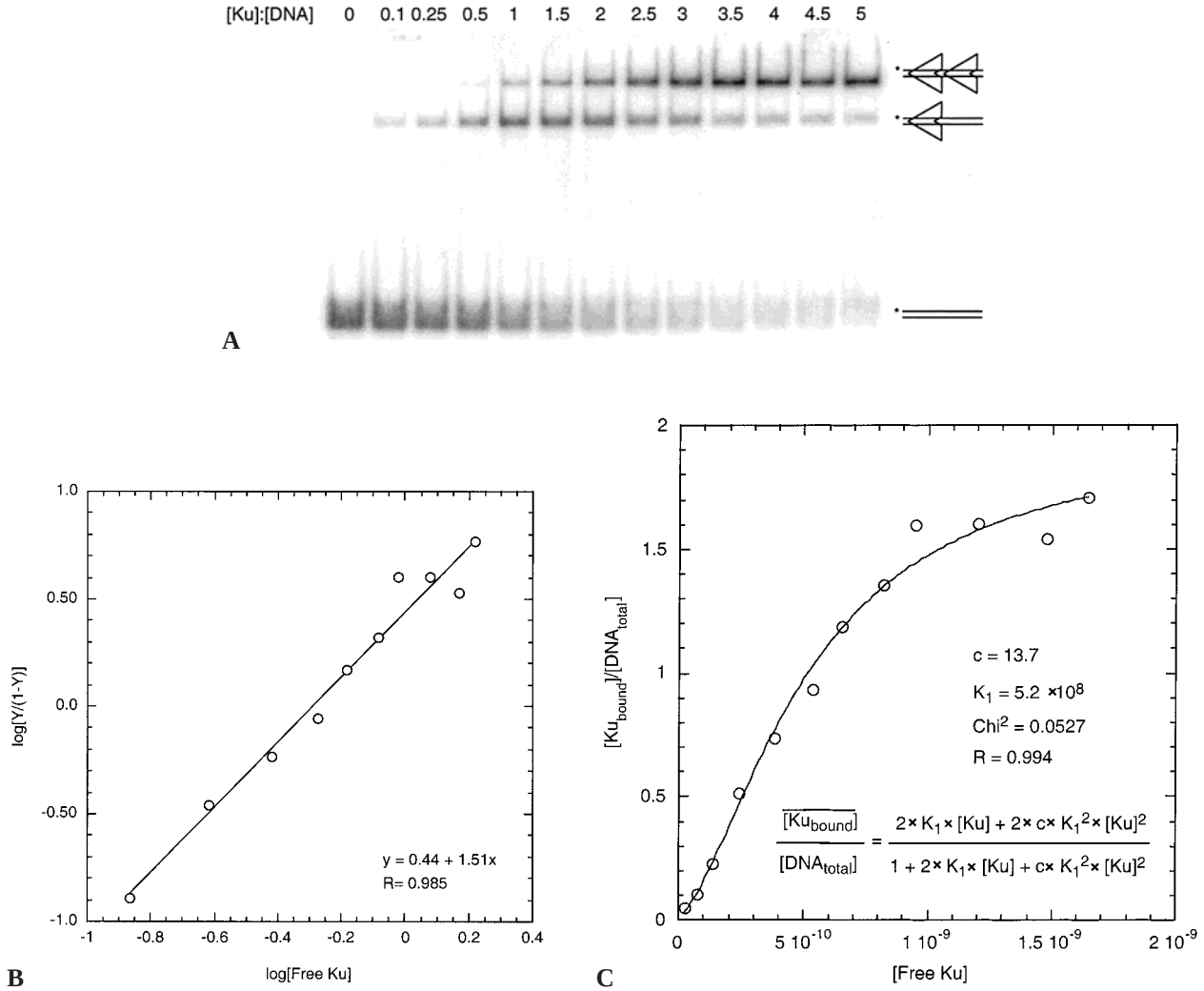


FIGURE 3: Ku binding to 45 bp ds DNA indicates cooperative binding. (A) EMSA of Ku binding to 45 bp DNA. The DNA concentration was 0.5 nM in all binding reactions while Ku concentrations are represented by the Ku to DNA ratios. Positions of the free probe, Ku:DNA, and $Ku_2$:DNA complexes are indicated ($Ku_2$:DNA complex has another configuration (see text)). (B) The Hill plot of the Ku EMSA (panel A) with the 45 bp DNA as a probe (see text). The formula represents the best-fit line for the data, and "R" is the regression coefficient. (C) Nonlinear curve fitting of EMSA data of Ku and 45 bp (panel A and see text). The equation used was indicated in the figure. $[Ku_{bound}]/[DNA_{total}]$ is plotted on the *y*-axis, [free Ku] is plotted on the *x*-axis, "$K_1$" is the intrinsic association constant of Ku binding to a 1-site DNA molecule, "*c*" is the cooperativity factor (see Experimental Procedures), "$chi^2$" is the residual, and "*R*" is the regression coefficient. Values for $K_1$ and *c* are for the best-fit curve.

Table 2: Kinetic Parameters of Ku Binding to DNA by SPR

| DNA | $k_a$ ($M^{-1}$ $s^{-1}$) | $k_d$ ($s^{-1}$) | $K_A$ ($M^{-1}$) | $K_D$ (M) | $Chi^2$ |
|---|---|---|---|---|---|
| 18 bp | $7.2 \times 10^6$ | $1.0 \times 10^{-2}$ | $7.0 \times 10^8$ | $1.4 \times 10^{-9}$ | 2.45 |
| 22 bp | $9.3 \times 10^6$ | $1.5 \times 10^{-3}$ | $6.3 \times 10^9$ | $1.6 \times 10^{-10}$ | 0.24 |
| 68 bp | $7.1 \times 10^6$ | $2.5 \times 10^{-4}$ | $2.8 \times 10^{10}$ | $3.6 \times 10^{-11}$ | 0.81 |

molecules could bind. We find that the association and dissociation kinetics fit a simple Langmuir binding model (Figure 5B). We observed this simple noncooperative behavior in three independent binding experiments and at a range of temperatures from our standard 25 °C down to temperatures as low as 12 °C (data not shown).

## DISCUSSION

*Positive Cooperativity in Ku Binding to 2-Site DNA Molecules.* A single Ku molecule binds noncooperatively and with simple Langmuir kinetics to linear ds DNA that is only one site size in length. However, we find that on DNA of sufficient length to accommodate two Ku molecules, positive cooperativity is detected in both EMSA and SPR assays. This cooperativity is not sequence dependent. Our data suggest that the second Ku molecule loads onto the DNA and subsequently forms additional physical contacts with the first Ku that is already present. If the second Ku were to make contact only with the first Ku (not the DNA) when loading, then one would see two Ku molecules bind even on 1-site DNA. However, this is not the case (Figure 1A). Our data are most consistent with a model in which the second Ku loads onto the DNA end and then establishes contacts with the first Ku, thereby stabilizing both Ku molecules (Figures 3 and 4).

It is interesting to note that the Hill coefficient in the simultaneous binding model is 1.6 instead of the theoretical maximal value of 2. This could be because Ku can load from either DNA end in the EMSA method. Most proteins would be expected to have a preferred face of loading. We speculate that if Ku binds with a preferred face, then some of the 45 bp ds DNA molecules containing two Ku molecules would have them oriented head-to-head and others would have them

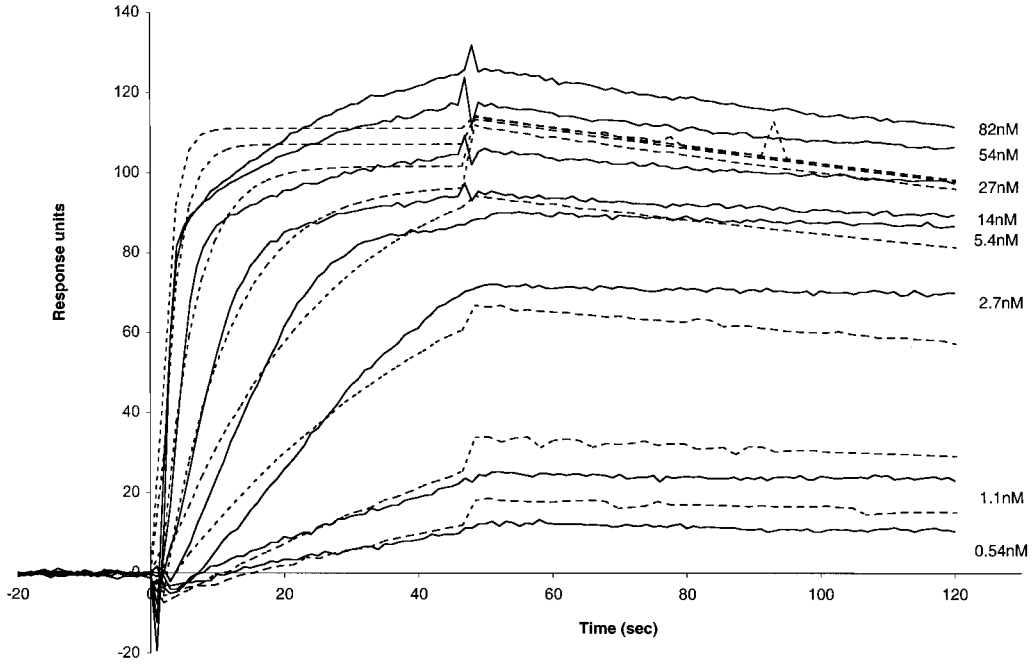


FIGURE 4: SPR Sensorgram of Ku binding to a 45 bp DNA which is terminally linked to the sensor chip surface. Single runs of eight Ku concentrations (82, 54, 27, 14, 5.4, 2.7, 1.1, and 0.54 nM) are shown. Dashed lines indicate the best-fit curves. Attempts to fit subsets of these eight curves (specifically the lower concentrations) still show significant deviations from the Langmuir model.

oriented head-to-tail (Figure 6). Cooperativity is likely to only occur for one, rather than both, of these two orientations. The $Ku_2$:DNA complexes with the Ku molecules loaded in a noncooperative manner may explain the observed Hill coefficient being less than the theoretical maximum of 2.

*Internal Ku Molecules May Not Interact Cooperatively.* Our kinetic and equilibrium data for 3- and 4-site DNA molecules raise the possibility that the internal Ku molecules interrupt the cooperative interactions with terminally bound Ku molecules. If so, Ku molecules bound to DNA may best be considered as two populations. One population of Ku molecules would consist of those bound at the DNA ends, and these can interact with one another cooperatively, perhaps only in a head-to-tail manner. The second population of Ku molecules would be those that are internally bound. These would not cooperatively interact with the Ku molecules of the first population. In fact, it has been suggested that the Ku molecules are not equivalent in a multimeric Ku−DNA complex (*25*).

It is important to note that it is difficult to assess the cooperative nature of the internal Ku molecules with absolute certainty. An alternative explanation for the noncooperative binding (EMSA and SPR) for 3- and 4-site DNA could be that the complexity of the system (with some species having unoccupied internal positions) may make it difficult to detect the small fraction of Ku:DNA species that are positioned in a manner that would permit cooperativity.

Interestingly, Ku binds to 18 bp, 22 bp, and 68 bp DNA with similar on-rates, reflected by similar $k_a$ values, but decreasing off-rates, reflected by decreasing $k_d$ values (Table 2). Since both 18 bp and 22 bp bind to one Ku molecule, the difference between the kinetics of Ku binding to these DNAs is probably because 18bp is slightly smaller than a full one-site DNA necessary to accommodate one Ku molecule. The slow off-rate of Ku from the 68 bp DNA may be contributed by the diffusion of Ku from an internal position to an end position. Therefore, the $k_d$ of Ku on the 68 bp DNA is only an apparent $k_d$ instead of the intrinsic $k_d$ of Ku to a DNA end.

*Physiologic Significance of the Interaction of Bound Ku Molecules.* One of the requirements of NHEJ is that the ends must be processed (i.e., remodeled) into a ligatable configuration before the XRCC4/DNA ligase IV complex can ligate the ends. During this remodeling phase, the two ends may transiently pair at partial regions of homology. There is genetic evidence that pairing of nonligatable end-to-end configurations can occur prior to at least one of the processing steps (*36*). It has been unclear how such pairing might occur. Bliss and Lane (*25*) provided data indicating that Ku could transiently move from one DNA end to another, but only if there was some degree of base pairing between the ends. (It is important to note that their experiments were done at 4 °C and that the transfers that they observed may be even more transient and difficult to observe at physiologic temperatures.) Given evidence for such transfers, a related question is whether one or more Ku molecules can cause two DNA ends to physically associate. We have been unable to observe any interaction of Ku molecules on different DNA molecules across 4 bp compatible junctions, even at low temperature (Ma, Y., and Lieber, M. R., unpublished). Nevertheless, there is some evidence for end-to-end associations between DNA molecules bound by Ku (*37*). Regardless of whether these transient end-to-end Ku transfers are observable in purified systems under physiologic conditions, they may occur transiently and intermittently in vivo. The cooperative interactions observed here may help in some end-to-end Ku:DNA configurations. In one such scenario, a Ku molecule could initially be bound at each of the two DNA ends at a ds DNA break. Upon transient base pairing between the two DNA ends, cooperative interaction between the two terminal Ku molecules may now facilitate end-to-end approximation long enough for

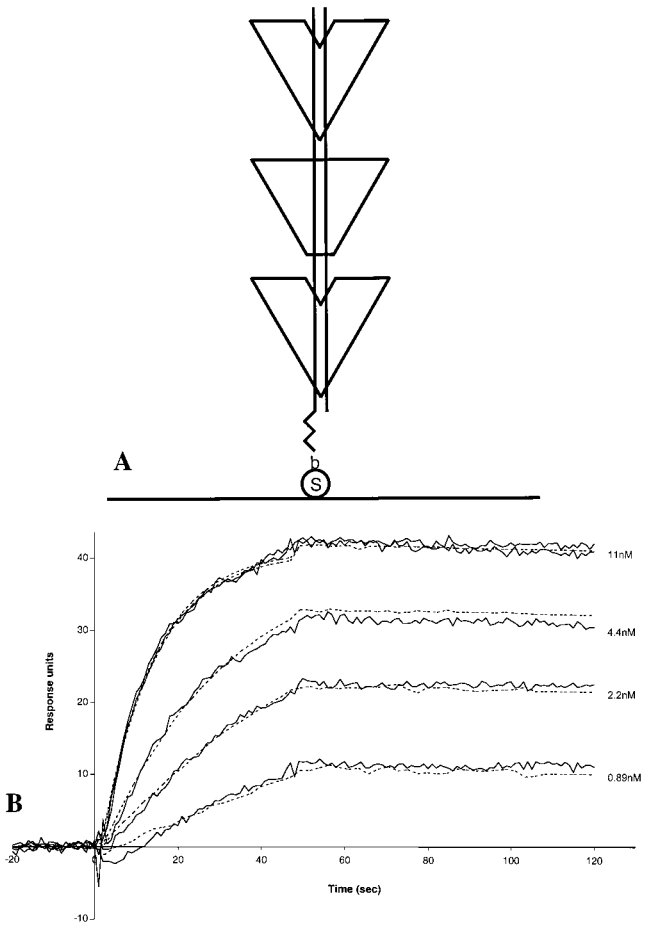


FIGURE 5: Ku binding to terminally linked 68 bp DNA indicates simple Langmuir interaction. (A) Diagram of the interaction of Ku with a 68 bp DNA, which is linked to the sensor chip surface at the DNA terminus. Terminally positioned Ku molecules are depicted as being capable of cooperative interaction while the internal Ku is represented by a noninteracting molecule. (B) SPR sensorgram of Ku binding to a 68 bp DNA which is linked to the sensor chip surface at the end. Single runs of four concentrations (11, 4.4, 2.2, and 0.89 nM) are shown. The binding of Ku at 11 nM was repeated once. Dashed lines indicate the best-fit curves. The dissociation phase was shortened for simplicity since this had no effect on the best-fit kinetic values. Biacore software curve-fitting program emphasizes the later portion of the association phase and the early portion of the dissociation phase.

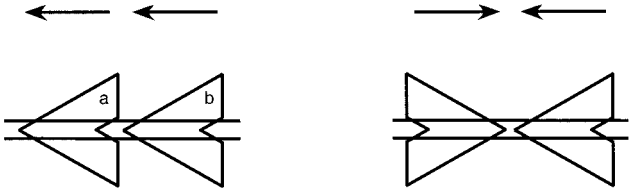


FIGURE 6: Possible configurations of the interaction of Ku with a 45 bp DNA. The arrows indicate the hypothetical directions of the loading of the Ku molecules. Thus, Ku(a) and Ku(b) are the first and second Ku molecules to load in the left diagram. On the right, each Ku molecule loads from its nearest DNA end.

ligation or further processing.

A second way in which cooperativity between terminal Ku molecules might play a physiological role is by providing more than one site for recruiting other factors that participate in or affect NHEJ. In addition to its interaction with the 469-kDa DNA-PK and WRN, Ku is known to interact with the histone acetylase, GCN5 (*38*) and with the XRCC4/DNA ligase IV complex (*39*, *40*). The presence of more than one Ku molecule at the incipient junction may be important in permitting the necessary factors to bind throughout the NHEJ process.

These are only two of several scenarios in which the features of Ku binding described here may influence the NHEJ process. Regardless of the specific role, the cooperative interaction for specific Ku:DNA configurations is an additional facet in that it is likely to be important in the progression of the NHEJ process through its several steps.

## ACKNOWLEDGMENT

We thank Dr. Timothy Lohman and John Hsieh (Washington University, St. Louis) for advice on the sequential binding analysis and initial guidance on the curve fitting program, respectively. We thank Kenneth Dickerson (Biocore, Inc.) for advice on the use of the Biocore instrument and software. We also thank Fred Chedin, Zarir Karanjawala, Kefei Yu, and Alex Taghva for comments on the manuscript.

## REFERENCES

1. Lieber, M. R. (1998) *Am. J. Path. 153*, 1323−1332.
2. Takata, M., Sasaki, M. S., Sonoda, E., Morrison, C., Hashimoto, M., Utsumi, H., Yamaguchi-Iwai, Y., Shinohara, A., and Takeda, S. (1998) *EMBO J. 17*, 5497−5508.
3. Karanjawala, Z. E., Grawunder, U., Hsieh, C.-L., and Lieber, M. R. (1999) *Curr. Biol. 9*, 1501−1504.
4. Gao, Y., Ferguson, D. O., Xie, W., Manis, J. P., Sekiguchi, J., Frank, K. M., Chaudhuri, J., Horner, J., DePinho, R. A., and Alt, F. W. (2000) *Nature 404*, 897−900.
5. Difilippantonio, M. J., Zhu, J., Chen, H. T., Meffre, E., Nussenzweig, M. C., Max, E. E., Ried, T., and Nussenzweig, A. (2000) *Nature 404*, 510−514.
6. Richardson, C., and Jasin, M. (2000) *Nature 405*, 697−700.
7. Yaneva, M., Kowalewski, T., and Lieber, M. R. (1997) *EMBO J. 16*, 5098−5112.
8. West, R. B., Yaneva, M., and Lieber, M. R. (1998) *Mol. Cell. Biol. 18*, 5908−5920.
9. Harrington, J. J., and Lieber, M. R. (1994) *EMBO J. 13*, 1235−1246.
10. Wilson, T. E., and Lieber, M. R. (1999) *J. Biol. Chem. 274*, 23599−23609.
11. Cooper, M. P., Machwe, A., Orren, D. K., Brosh, R. M., Ramsden, D., and Bohr, V. A. (2000) *Genes Dev. 14*, 907−912.
12. Li, B., and Comai, L. (2000) *J. Biol. Chem. 275*, 28349−28352.
13. Grawunder, U., Wilm, M., Wu, X., Kulesza, P., Wilson, T. E., Mann, M., and Lieber, M. R. (1997) *Nature 388*, 492−495.
14. Schar, P., Herrmann, G., Daly, G., and Lindahl, T. (1997) *Genes Dev. 11*, 1912−1924.
15. Teo, S.-H., and Jackson, S. P. (1997) *EMBO J. 16*, 4788−4795.
16. Featherstone, C., and Jackson, S. P. (1999) *Mutat. Res. 434*, 3−15.
17. Gao, Y., Chaudhurri, J., Zhu, C., Davidson, L., Weaver, D. T., and Alt, F. W. (1998) *Immunity 9*, 367−376.
18. Gu, Y., Sekiguchi, J., Gao, Y., Dikkes, P., Frank, K., Ferguson, D., Hasty, P., Chun, J., and Alt, F. W. (2000) *Proc. Natl. Acad. Sci. U.S.A. 97*, 2668−2673.
19. Mimori, T., and Hardin, J. A. (1986) *J. Biol. Chem. 261*, 10375−10379.
20. Paillard, S., and Strauss, F. (1991) *Nucl. Acids Res. 19*, 5619−24.
21. Zhang, W.-W., and Yaneva, M. (1992) *Biochem. Biophys. Res. Commun. 186*, 574−579.

22. de Vries, E., van Driel, W., Bergsma, W. G., Arnberg, A. C., and van der Vliet, P. C. (1989) *J. Mol. Biol. 208*, 65−78.
23. Falzon, M., Fewell, J. W., and Kuff, E. L. (1993) *J. Biol. Chem. 268*, 10546−10552.
24. Smider, V., Rathmell, W. K., Brown, G., Lewis, S., and Chu, G. (1998) *Mol. Cell. Biol. 18*, 6853−6858.
25. Bliss, T. M., and Lane, D. P. (1997) *J. Biol. Chem. 272*, 5765−5773.
26. Gravel, S., Larrivee, M., Labrecque, P., and Wellinger, R. J. (1998) *Science 280*, 741−744.
27. Martin, S. G., Laroche, T., Suka, N., Grunstein, M., and Gasser, S. M. (1999) *Cell 97*, 621−633.
28. Hsu, H.-L., Gilley, D., Blackburn, E. H., and Chen, D. J. (1999) *Proc. Natl. Acad. Sci. U.S.A. 96*, 12454−12458.
29. Tuteja, N., Tuteja, R., Ochem, A., Taneja, P., Huang, N. W., Simoncsits, A., Susic, S., Rahman, K., Marusic, L., Chen, J., Zhang, J., Wang, S., Pongor, S., and Falaschi, A. (1994) *EMBO J. 13*, 4991−5001.
30. Ono, M., Tucker, P. W., and Capra, J. D. (1994) *Nucleic Acids Res. 22*, 3918−3924.
31. Blier, P. R., Griffith, A. J., Craft, J., and Hardin, J. A. (1993) *J. Biol. Chem. 268*, 7594−7601.
32. Knuth, M. W., Gunderson, S. I., Thompson, N. E., Strasheim, L. A., and Burgess, R. R. (1990) *J. Biol. Chem. 265*, 17911−17920.
33. Cornish-Bowden, A. (1979) *Fundamentals of Enzyme Kinetics*, Butterworths, London.
34. McGhee, J. D., and von Hippel, P. H. (1974) *J. Mol. Biol. 86*, 469−489.
35. Yoo, S., Kimzey, A., and Dynan, W. S. (1999) *J. Biol. Chem. 274*, 20034−20039.
36. Wu, X., Wilson, T. E., and Lieber, M. R. (1999) *Proc. Natl. Acad. Sci. U.S.A. 96*, 1303−1308.
37. Ramsden, D. A., and Gellert, M. (1998) *EMBO J. 17*, 609−614.
38. Barlev, N. A., Poltoratsky, V., Owen-Hughes, T., Ying, C., Liu, L., Workman, J. L., and Berger, S. L. (1998) *Mol. Cell. Biol. 18*, 1349−1358.
39. Nick McElhinny, S. A., Snowden, C. M., McCarville, J., and Ramsden, D. A. (2000) *Mol. Cell. Biol. 20*, 2996−3003.
40. Chen, L., Trujillo, K., Sung, P., and Tomkinson, A. E. (2000) *J. Biol. Chem. 275*, 26196−26205.

BI010932V